# Variation in Quantitative Myocardial Perfusion Due to Arterial Input Selection

Andres F. Vasquez, MD, Nils P. Johnson, MD, MS, K. Lance Gould, MD

*Houston, Texas*

**OBJECTIVES** This study compared the clinical implications of quantifying myocardial perfusion among different potential arterial input sites: the high (HAo) and basal (BAo) ascending aorta, descending aorta (DA), left atrium (LA), and left ventricular (LV) cavity.

**BACKGROUND** Absolute myocardial perfusion and its hyperemic reserve imaged by positron emission tomography (PET) can serve as noninvasive functional measures of physiologic severity. Quantitative myocardial perfusion by PET depends on the time– concentration of vascular activity, called *arterial input* (AI). However, arterial activity imaged by PET can vary among sites due to partial volume effects from anatomic size, cardiac or respiratory motion out of fixed regions of interest, and spillover from neighboring vascular structures.

**METHODS** Patients underwent cardiac rubidium-82 PET imaging with flow quantification using various anatomic AI. After excluding sites with overt spillover or misregistration, we selected the customized, highest AI among the BAo, HAo, DA, and LA. Average whole heart flows and percent of LV with substantial definite ischemia were compared among sites.

**RESULTS** Of 288 cases, LA was selected in roughly half, with HAo in another quarter to one-third. Compared with using the customized AI, rest and stress absolute flow were higher by 5% to 10% for HAo, 14% for BAo, 19% to 23% for DA, and 46% to 49% for LV due to artifactually low AI values. The ratio of coronary flow reserve to its customized value was less affected, although its 95% confidence interval increased among AI locations: 7% for LA, 16% for HAo, 20% for BAo, 28% for DA, and 31% for LV.

**CONCLUSIONS** The best customized site for AI activity varies for each patient among potential anatomic locations. Selection of the customized arterial site for each individual improved quantification of myocardial perfusion and coronary flow reserve with less variability compared with utilizing a single, pre-selected, fixed anatomic site. (J Am Coll Cardiol Img 2013;6:559–68) © 2013 by the American College of Cardiology Foundation

Coronary mechanical revascularization guided by a functional measure of stenosis severity produces better outcomes than when guided by anatomic percent diameter stenosis (1). Absolute myocardial perfusion in units of flow per tissue mass (cc/min/g) can identify hyperemic low-flow and coronary flow reserve (CFR) thresholds associated with ischemia as analogous, noninvasive functional measures of physiologic severity (2,3). Quantitative myocardial perfusion by positron emission tomography (PET) depends on the time–concentration of vascular activity, called *arterial input* (AI).

Many potential anatomic locations for quantification of AI exist, including the aorta, left atrium (LA), and left ventricular (LV) blood pool. These sites show similarly shaped radiotracer concentration time–activity curves. However, substantial heterogeneity among them (4) arises from a combination of statistical noise, differential partial volume effects, varying attenuation correction based on coregistration of emission and transmission images, respiratory and cardiac motion during image acquisition, and potential spillover of activity from adjacent vascular structures.

In a group of patients, myocardial blood flow (MBF) and CFR have distributions of values due to biologic variability. However, in an individual patient, variables intrinsic to that patient alter arterial activity recovery when quantifying absolute flow. These intrinsic variables are unpredictable and difficult or impossible to measure and correct on a per-patient basis in routine clinical practice. These variables most commonly decrease arterial count recovery from its true value, except for spillover and emission/attenuation misregistration that increase apparent arterial activity. Consequently, a "single-location-fits-all" approach using a pre-selected fixed arterial site may lead to decreased arterial count recovery in a significant number of patients. Due to the nonlinear relationship between flow and uptake for most radiotracers, small changes in the arterial activity input to perfusion models are magnified into larger differences in absolute flow. AI recovery below its true value leads to an overestimation of absolute perfusion, thereby underestimating the severity of flow re-striction throughout the myocardium. For arterial sites with spillover or misregistration contamination, the AI appears higher than its true value, thereby causing erroneously low flow values and flow restriction severity overestimation.

We define that the best customized AI for each patient recovers the highest arterial activity among potential anatomic locations when using a small region of interest (ROI) and excluding sites with overt spillover and misregistration overcorrection. We consequently hypothesized that the customized AI determined for each individual rest and stress image reduces variability in quantification of myocardial perfusion compared with utilizing a pre-selected, single, fixed anatomic site.

## METHODS

Subjects underwent myocardial perfusion PET with absolute flow quantification for potential or known coronary artery disease (CAD) at the Weatherhead PET Center for Preventing and Reversing Atherosclerosis of the University of Texas Medical School at Houston and Memorial Hermann Hospital. They gave written informed consent approved by the institutional review board.

**PET acquisition protocol and image reconstruction.** Patients were instructed to fast for 4 h and to abstain from caffeine, theophylline, and cigarettes for 24 h before the study. Imaging was performed in the vast majority of cases (just over 80%) using a Discovery ST scanner with hybrid 16-slice computed tomography (CT) (GE Healthcare, Waukesha, Wisconsin) operating in 2-dimensional (2D) mode with a resolution full-width half maximum of 6.28 mm at 1 cm off axis as previously described (2,3,5). For comparative purposes, a Positron mPower rotating-rod scanner (Positron Corporation, Fishers, Indiana) operating in 2D mode was used for a minority of cases (just under 20%) with no difference in average CFR. Decay and scatter correction were performed. Rest emission data were obtained over 7 min after injection of 1,295 to 1,850 MBq (35 to 50 mCi) of generator-produced rubidium-82 (Bracco Diagnostics, Princeton, New Jersey). Emission image acquisition started at the instant the generator began flushing tracer toward the patient, with an arrival delay of 8 to 15 s depending on the age of the generator.

Immediately after completion of the resting scan, dipyridamole (142 μg/kg/min) was infused for 4 min. Four minutes after the completion of dipyridamole infusion, the same dose of radiotracer was

given. Emission image acquisition was started immediately. The first 2 min of the emission images were binned to form the AI data. The last 5 min of the emission images were binned to form the myocardial uptake data. CT or rotating-rod scans for attenuation correction were acquired before rest and after stress imaging as previously reported (6).

GE images were reconstructed using filtered back projection with a ramp filter (cutoff = 6.5 mm) and then post-processed by a fifth-order Butterworth filter (cutoff = 0.50 cycles/cm). Positron images were reconstructed using filter back projection with a ramp filter multiplied by a fifth-order Butterworth apodizing window function (cutoff = 0.04 cycles/mm). Fused emission and attenuation images optimized coregistration by shifting as needed. After reconstruction, a 3-dimensional rotation algorithm generated true short- and long-axis views of the LV from transaxial images using previously described quantitative software (2,3). Circumferential profiles of maximum LV radial activity for each true short-axis slice were used to construct 2D topographic views (lateral, inferior, septal, and anterior LV quadrant views) of 64 radial pixels for each of 21 short-axis slices, as previously described.

**Quantitative PET image analysis.** Arterial activity was determined from transaxial images by selecting the highest activity using a 2.5-mm–diameter (compared with the reconstructed isotropic voxel dimensions of 3.27 mm on each side) circular ROI on a single slice in the LA, basal ascending aorta (BAo), high ascending aorta (HAo), and descending aorta (DA) during the first 2 min after each radiotracer injection. The ROI in the DA was chosen in its mid-portion to avoid spillover from adjacent pulmonary artery activity or attenuation over-correction due to local aortic misregistration when aligning the myocardium, both of which often cause artifacts for the most proximal and/or most distal portions. An ROI was placed in the center of the LV cavity on the early uptake images, then copied onto the late myocardial uptake LV images at identical coordinates (left ventricular copied ROI [LVBP]).

To assess potential spillover from myocardium or myocardial motion into the fixed LV blood pool ROI, two additional ROI sites were selected in a subgroup of 25 patients, as follows: 1) highest activity in the basal LV cavity (LV highest) on early blood pool images while avoiding high activity close to or within myocardium; and 2) an LA ROI positioned on late images, then copied onto early arterial images (left atrial copied ROI [LABP]).

For this subset of 25 patients, these two ROI sites (LV highest and LABP) were in addition to the same arterial activities described above for all patients. Thus, for this subgroup, there were 2 LA and 2 LV ROI sites—LV and LV highest, and LA and LABP.

Erroneously high ROI values may result from spillover or positioning over the myocardium that is poorly delineated on early images and subject to contractile or translational movement, particularly during tachycardia of stress, when systole accounts for a greater proportion of the heart cycle. Therefore, the highest AI site was selected in each patient separately for rest and stress from the LA, BAo, HAo, and DA and termed the *customized AI* after excluding sites compromised by visibly overt spillover from adjacent structures or misregistration. In such cases, the next-highest AI site was selected.

For each radial segment of every short-axis slice, AI and myocardial uptake were used to compute absolute myocardial flow using an established model (7) implemented using custom software. The flow model does not use time–activity curves but instead integrates AI over the first 2 min of the early "arterial" image. Partial volume corrections were based on quantitative phantom studies specific for each scanner (GE: arterial 1.0, myocardial 0.9; Positron: arterial 1.166, myocardial 0.7), as derived previously (8). The topographic map of absolute flow was smoothed using a 5-by-5 pixel average to suppress noise introduced by the flow model. CFR was computed as the stress-to-rest ratio on a pixel basis.

Myocardium with flow capacity below the limits of definite ischemia (2,3) was recorded by software (stress flow ≤0.91 cc/min/g; CFR ≤ 1.74). A severe perfusion defect was defined as at least 10% of the LV with definite ischemia. In two patients, true coincidence counts of first-pass activity were divided into eight equal-sized temporal R-R bins by electrocardiography gating to evaluate displacement of arterial activity pools during the cardiac cycle relative to a fixed arterial ROI.

**Statistical methods.** All statistical analyses were performed using R version 2.15 (R Foundation for Statistical Computing, Vienna, Austria). Continuous variables are summarized as mean ± SD, or median (interquartile range) for non-normal distributions. Frequency variables are summarized as number (percent) and were compared using a chi-square test. Analysis of variance (ANOVA) from a linear mixed-effects model with random effects within subjects assessed changes in absolute flow

and CFR. If this ANOVA was significant, then a Tukey all-pair comparison was performed to determine which AI locations were different. Box plots identify outliers as 1.5 times the interquartile range. All applicable tests were 2-tailed, and p < 0.05 was considered statistically significant.

## RESULTS

Figure 1 demonstrates an example case of contrasting clinical interpretations due to noncustomized AI selection. Figure 2 illustrates an example of ROI placement for each potential AI site.

No significant difference in average CFR existed between GE and Positron scanners (2.68 ± 0.79 vs. 2.47 ± 0.83; p = 0.09). For all 288 cases, Table 1 quantifies the effect of noncustomized AI selection on absolute flow and CFR when applying a "one-size-fits-all" strategy. Average values describe the typical bias from the customized ROI location,

while the 95% confidence interval (CI) quantifies the variation of values. Although CFR is less affected by a noncustomized ROI location than rest and stress flow, its 95% CI widens from 7% (0.96 to 1.03) when using the LA to 31% (0.86 to 1.17) when using the LV cavity.

Figure 3 compares the distribution of AI at rest and stress among AI locations. As detailed in Table 2, the customized AI location occurred most frequently in the LA (roughly half of cases) and HAo (another fourth to one-third of cases). Always selecting the HAo would reduce the median AI by 3% to 5%, while always selecting the LV cavity would reduce it by 17% to 18%. The 95% CIs widen in Table 2 with less-customized ROI locations.

Figures 4 and 5 compare the distributions of rest flow, stress flow, and CFR among AI locations. Table 3 compares AI and flow among potential ROI locations. The percentage of cases with siz-
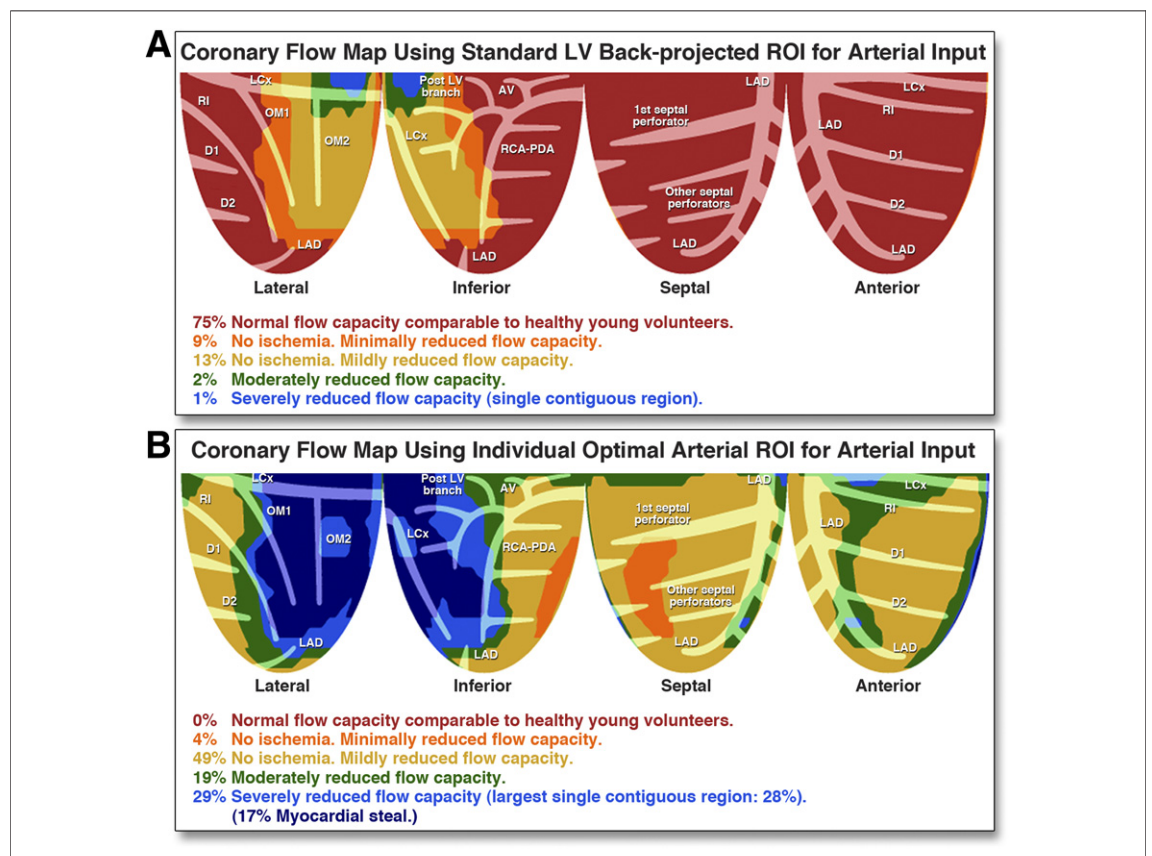


**Figure 1. Clinical Impact of Copied Versus Customized AI**

Comparison of flow maps (3) in the same patient using the standard copied arterial input (AI) location from the late image **(A)** versus the customized location **(B)**. Alternative AI values increase flows and lead to different clinical interpretations of identical, raw imaging data. AV = atrioventricular; D1 = 1st diagonal; D2 = 2nd diagonal; LAD = left anterior descending; LCx = left circumflex; LV = left ventricle; OM1 = 1st obtuse marginal; OM2 = 2nd obtuse marginal; PDA = posterior descending artery; RCA = right coronary artery; RI = ramus intermedius; ROI = region of interest.

able, definite ischemia differed among ROI locations (chi-square p value = 0.007). Absolute flow and CFR differed among anatomic locations (ANOVA from linear mixed-effects model p values <0.001 for rest flow, stress flow, and CFR). All rest flows differed from each other (Tukey p value ≤0.001) except HAo versus LA (Tukey p value = 0.055). All stress flows differed from each other (Tukey p value <0.001) except BAo versus HAo (Tukey p value = 0.37) and DA (Tukey p value = 0.14). However, CFR only differed between HAo and BAo (Tukey p value = 0.043) and DA (Tukey p value <0.001) and LA (Tukey p value = 0.002) and between DA and LV (Tukey p value = 0.001).

On gated first-pass images, LV blood pool moved into and out of the fixed, copied LV ROI due to substantial contractile and translational motion during the cardiac cycle. Figure 6 demonstrates the basis for LV blood pool variability due to myocardial translation into the ROI. Consequently, Tables 1 and 2 demonstrate the widest CIs for the LV cavity among all potential ROI locations compared with the customized AI.

Sites with overt spillover occurred in 3.5% of BAo and 3.6% of HAo cases. Misregistration artifacts occurred in 9.2% of DA cases. In the subset of 25 cases, selecting the ROI in the LV blood pool with highest AI systematically overestimated the customized stress AI by 5.4%. In contrast, the LVBP underestimated the customized stress AI by 17%. Similarly, using the LABP underestimated the customized stress AI by 17%.

## DISCUSSION

Our results support several conclusions. First, AI variability among different arterial sites has significant impact on quantifying absolute myocardial perfusion. Second, a "one-location-fits-all" approach using a fixed, pre-selected, single AI site underestimates or overestimates MBF in significant numbers of patients. The best site for AI varies for each patient and at times between rest and stress for the same patient. Third, our data suggest the following guidelines for customized AI selection to quantify myocardial perfusion accurately:

1. Place ROIs at multiple sites in the aorta (ascending and descending) and LA using a small ROI. Select the site with highest arterial activity after excluding poorly delineated sites, those with significant spillover observed from adjacent high activity structures, and those with
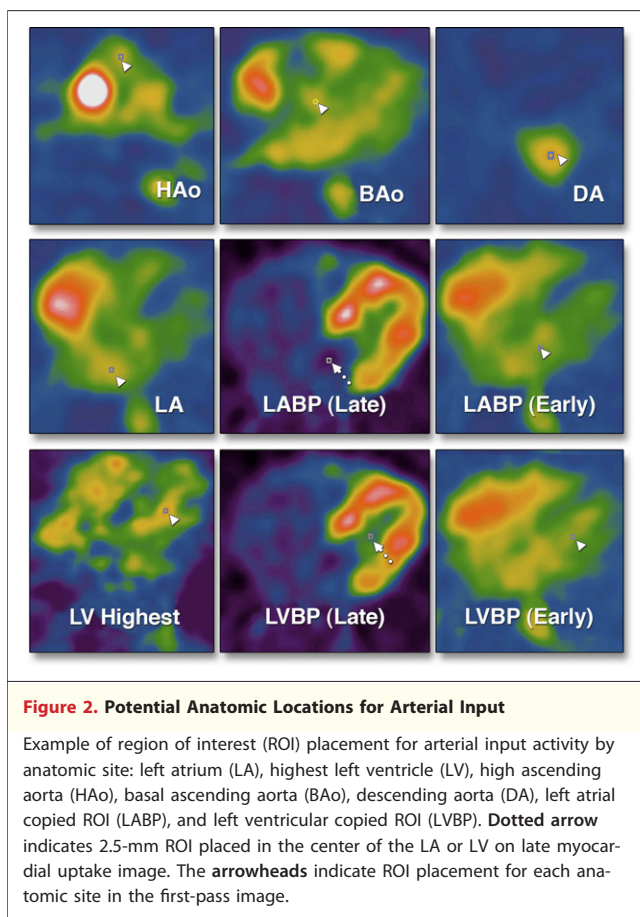


**Figure 2. Potential Anatomic Locations for Arterial Input**

Example of region of interest (ROI) placement for arterial input activity by anatomic site: left atrium (LA), highest left ventricle (LV), high ascending aorta (HAo), basal ascending aorta (BAo), descending aorta (DA), left atrial copied ROI (LABP), and left ventricular copied ROI (LVBP). **Dotted arrow** indicates 2.5-mm ROI placed in the center of the LA or LV on late myocardial uptake image. The **arrowheads** indicate ROI placement for each anatomic site in the first-pass image.

misregistration artifacts, particularly overcorrection of DA activity.

2. The LV blood pool is frequently contaminated by significant early myocardial uptake via spillover and translation. Therefore, selecting the highest LV AI frequently leads to underestimation of MBF and should be excluded. A copied ROI in the center of the LV cavity systematically overestimates myocardial flow due to underestimated AI caused by translational and contractile motion out of the fixed, LVBP during the cardiac cycle.

3. Customized selection of AI site is essential for accurate flow quantification in individual patients as the guide for revascularization and management decisions in patients with coronary artery disease.

We chose a 2.5-mm–diameter circular ROI for AI quantification, as a small ROI is more likely to identify the true count peak independent of spreading effects from positron range and the imaging system, and it may be more easily distanced from spillover sources. The LA offers the best count

**Table 1. Consequence of Noncustomized AI on Myocardial Flow**

|  | Rest | Stress | CFR |
|---|---|---|---|
| Customized | 1.00 | 1.00 | 1.00 |
| Left atrium | 1.00 (1.00–1.09) | 1.00 (1.00–1.08) | 1.00 (0.96–1.03) |
| High ascending aorta | 1.05 (1.00–1.16) | 1.10 (1.00–1.22) | 1.01 (0.96–1.12) |
| Low ascending aorta | 1.14 (1.05–1.25) | 1.14 (1.03–1.23) | 1.00 (0.90–1.10) |
| Descending aorta | 1.23 (1.12–1.32) | 1.19 (1.04–1.30) | 0.97 (0.89–1.07) |
| Left ventricular cavity | 1.49 (1.31–1.67) | 1.46 (1.30–1.70) | 0.99 (0.86–1.17) |

Values are median ratios (95% confidence interval) of left ventricular flow to customized flow.
AI = arterial input; CFR = coronary flow reserve.

recovery in a majority of cases, suggesting that it is less affected by the interplay of spillover, partial volume loss, misregistration, and translation compared with other sites. On gated images, the DA demonstrated least translation yet had the lowest AI of all groups, likely due to larger partial volume loss resulting from the smaller anatomic diameter of the DA.

The effect of spillover is most pronounced between the LV blood pool and LV myocardial activity, where both areas contaminate each other. Myocardial activity recovery increases during the tachycardia of dipyridamole stress, as systole occupies a greater portion of the cardiac cycle compared with rest resulting in less partial volume loss (9). This greater portion of the cardiac cycle in systole with higher activity recovery than at rest augments spillover into the LV blood pool, with correspond-

ing underestimation of stress flow when using the highest LV AI. Thus, in the subset of 25 patients, at-rest LV highest was only 1% higher than the LA AI but during stress this difference increased to 9.5%. The largest single per patient difference of the LV highest compared with LA activity was 25% at rest up to 84% during stress, indicating great variability that is clinically more important than the significant but modest average rest-stress differences noted above.

Potential spillover sources exist for every AI location: BAo from the adjacent right atrium, right ventricle and septal myocardium; HAo from the superior vena cava and pulmonary artery; high LA from the right lower pulmonary artery; lower and rightward LA from the right atrium and inferior vena cava reflux and the LV myocardium toward the basal LA. It is therefore important to select a central LA location and avoid "hot spots" that represent adjacent structures or are significantly polluted by spillover from these neighboring structures.

The DA is least prone to spillover contamination. However, it is adjacent to vertebral bones, causing upward over-correction of activity due to smearing of attenuation correction associated with limited resolution or due to PET/CT misregistration correction that shifts the bone-attenuation correction over the DA when properly aligning the LV myocardium. Misregistration-related over-correction was most notable toward the more distal
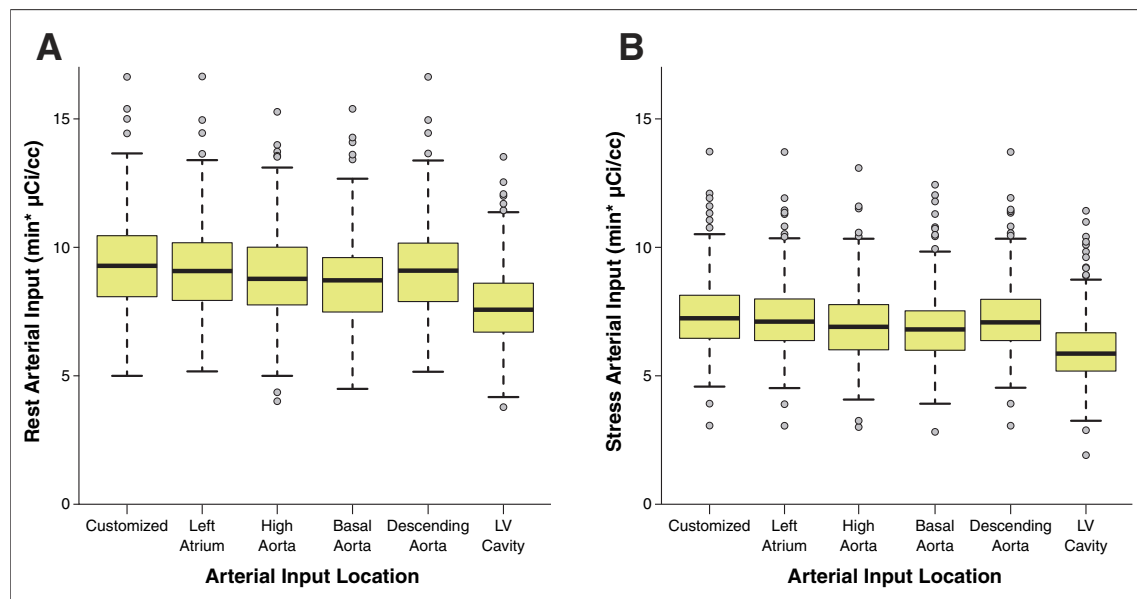


**Figure 3. Variation of AI Among Anatomic Locations**

Box plots of rest (A) and stress (B) AI by anatomic site. **Thick horizontal line** denotes the median centered in a box from the 25th to the 75th quartile, with **vertical bars** extending to ±1.5 times the interquartile range. Abbreviations as in Figure 2.

**Table 2. Distribution of Customized AI Locations and Values**

| ROI Location | Customized AI, N (%) | | Median Ratio (95% CI) of AI to Customized AI | |
| --- | --- | --- | --- | --- |
| | Rest | Stress | Rest | Stress |
| Left atrium | 139 (48) | 150 (52) | 1.00 (0.95–1.00) | 1.00 (0.96–1.00) |
| High ascending aorta | 93 (32) | 69 (24) | 0.97 (0.93–1.00) | 0.95 (0.90–1.00) |
| Low ascending aorta | 37 (13) | 30 (10) | 0.93 (0.90–0.98) | 0.93 (0.90–0.98) |
| Descending aorta | 19 (7) | 39 (14) | 0.90 (0.87–0.95) | 0.91 (0.88–0.98) |
| Left ventricular cavity | 0 (0) | 0 (0) | 0.83 (0.78–0.87) | 0.82 (0.76–0.87) |

AI = arterial input; CI = confidence interval; ROI = region of interest.

portions of the DA. We therefore avoided the most distal transaxial slices and those with obvious partial volume over-correction that had significantly higher AI than to other sites or as high as the pulmonary artery.

During tachycardia, systole occupies a larger proportion of the cardiac cycle compared with rest. Consequently, dipyridamole stress increases displacement of adjacent myocardium into and out of a fixed LV ROI and limits reliable identification of the LV ROI uncontaminated by adjacent myocardial activity. Copying an ROI from the late images to the early images fails to identify the ROI with best arterial count recovery due to blood pool moving out of the fixed, copied LV ROI. Consequently, the LVBP site systematically overestimates blood flow as demonstrated by LVBP and LABP both underestimating stress AI compared with the

customized value. The DA and HAo show the least translation as they are somewhat fixed by ligaments or retroperitoneum.

We found significant translation of all potential AI sites on electrocardiographic gated images during the first 2 min after intravenous injection. However, for all sites except the LV, the extent of motion or translation was not larger than the anatomic arterial site so that a small central ROI captured the true maximal activity in at least one of the arterial sites having no spillover or misregistration. Nonetheless, translation was more pronounced in the LV where the myocardium as well as low count segments of the blood pool moved substantially into or out of the fixed LV ROI as illustrated in Figure 6, highlighting the intrinsic variability of this site. The descending aorta was least affected by translation during analysis of the
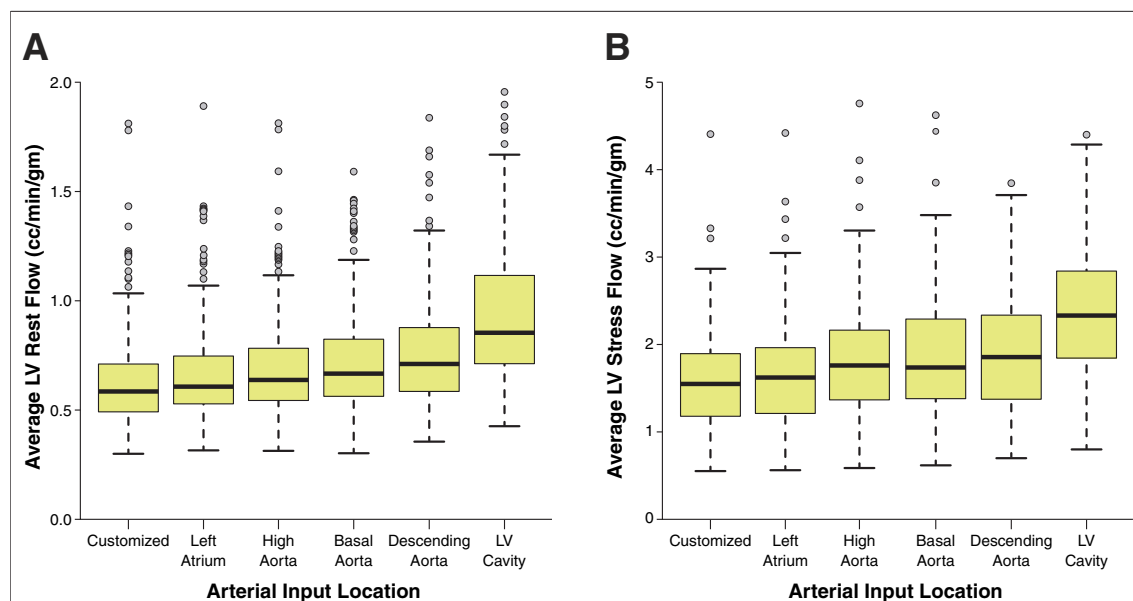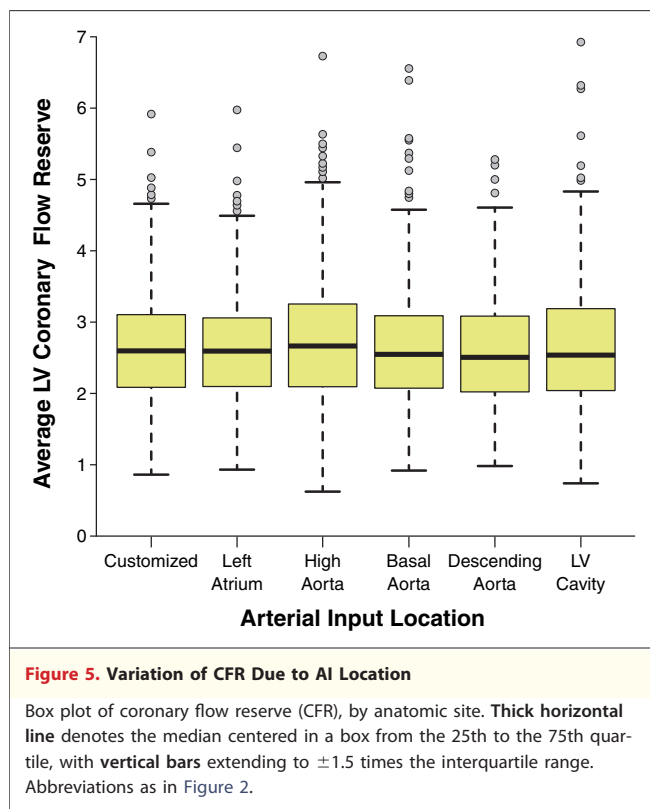


**Figure 4. Variation of Absolute Flow Due to AI Location**

Box plots of rest **(A)** and stress **(B)** whole myocardial blood flow by anatomic site. **Thick horizontal line** denotes the median centered in a box from the 25th to the 75th quartile, with **vertical bars** extending to ±1.5 times the interquartile range. Abbreviations as in Figure 2.

**Figure 5. Variation of CFR Due to AI Location**

Box plot of coronary flow reserve (CFR), by anatomic site. **Thick horizontal line** denotes the median centered in a box from the 25th to the 75th quartile, with **vertical bars** extending to ±1.5 times the interquartile range. Abbreviations as in Figure 2.

AI value is not limited by low counts or greatly influenced by statistical variations, unlike time–activity curve methods. Additionally, a single voxel ROI for the AI actually represents the average over a much larger volume due to the finite resolution of the PET scanner.

**Comparison to existing literature.** Limited data exist on variability of quantitative perfusion due to AI site selection. LA activity recovery is reportedly similar to activity measured directly from arterial samples (7), suggesting that partial volume correction may not be a significant issue in the LA. Both the LA and LV reportedly have similar activity recovery within 3% for oxygen-15 carbon monoxide equilibrium analysis (9).

LA blood arterial time–activity curves closely approximate arterial–time activity curves obtained by direct blood sampling from the femoral artery, with MBF derived from a 2-compartment model that matched microsphere data in a dog model (10). This experimental data is consistent with our findings that the LA is the most common location for the customized LA. However, patients are more variable anatomically and physiologically than the well-defined, controlled, experimental models, thereby making other arterial sites better in some patients.

In a smaller study, time–activity curves obtained by placing ROIs in the LA demonstrated sharper and higher peak time–activity curves than did the LV or the aorta, suggesting a variable trend toward better count recovery in the LA (11). Our larger data set definitively documents these findings but adds essential information on variability that precludes using any one pre-selected, fixed, constant arterial site for AI. For individual cases in our study, the highest activity or customized arterial site for AI was variable and unpredictably scattered among all arterial sites.

Myocardial spillover contamination of AI in the LV was found compared with the LA using oxygen-15 water (12). In 31 patients studied using

gated images in our patients but was more commonly small enough to have larger partial volume losses than were other sites.

A key difference exists between our integrative flow model (7) and typical time–activity curve fitting. Statistical noise is indeed high for usual 8- to 10-s PET images necessary to create a time–activity curve. However, our arterial image is acquired over the first 2 min after tracer injection, approximately 10-fold longer. Therefore, because the signal/noise ratio increases with the square root of the number of counts, our arterial images have approximately a 3-fold higher signal/noise ratio compared with time–activity curves. As such, our

**Table 3. Arterial Input and Flow by Anatomic Location**

|  | Input (µCi/cc · min) | | Flow (cc/min/g) | | | |
|---|---|---|---|---|---|---|
|  | **Rest** | **Stress** | **Rest** | **Stress** | **CFR** | **Ischemia*** |
| Customized | 9.29 (8.12–10.46) | 7.25 (6.51–8.15) | 0.58 (0.49–0.71) | 1.55 (1.18–1.91) | 2.64 ± 0.80 | 61 (21) |
| Left atrium | 8.80 (7.79–10.02) | 6.92 (6.07–7.80) | 0.64 (0.54–0.78) | 1.77 (1.37–2.17) | 2.75 ± 0.96 | 49 (17) |
| High ascending aorta | 8.72 (7.53–9.62) | 6.84 (6.02–7.58) | 0.67 (0.57–0.83) | 1.74 (1.38–2.30) | 2.65 ± 0.91 | 53 (18) |
| Low ascending aorta | 8.43 (7.34–9.43) | 6.79 (5.98–7.53) | 0.71 (0.58–0.88) | 1.86 (1.38–2.33) | 2.56 ± 0.79 | 52 (18) |
| Descending aorta | 9.09 (7.94–10.21) | 7.12 (6.41–8.00) | 0.61 (0.53–0.75) | 1.62 (1.21–1.97) | 2.62 ± 0.78 | 60 (21) |
| Left ventricle cavity | 7.59 (6.73–8.62) | 5.87 (5.22–6.68) | 0.86 (0.72–1.12) | 2.34 (1.84–2.85) | 2.69 ± 0.99 | 29 (10) |

Values are median (95% CI), mean ± SD, or n (%). *Defined as having ≥10% of the left ventricular with both stress flow <0.91 ml/min/g and CFR <1.74 (2,3).
CI = confidence interval; CFR = coronary flow reserve.

nitrogen-13 ammonia, the LV compared with the LA for AI had notable myocardial spillover leading to an average 8% underestimation of MBF, but up to 40% underestimation in individuals (9).

**Study limitations.** A potential limitation of our proposed method might be increased processing time and complexity. However, using semi-automated software developed by our group, the time spent to identify and select the customized AI site was on average 2 to 3 min per patient, with virtually instantaneous display of absolute perfusion, CFR, and flow capacity in 2D maps with color coding relative to low flow threshold causing ischemia (2,3). The software also extrapolates the ROI on early first-pass images onto late myocardial images for confirming the arterial ROI in relation to high-quality myocardial images. Completely automated ROI selection based on these manually applied principles could be developed in the future.

Currently no gold standard exists for quantifying myocardial flow in humans. Our definition of a "gold standard" AI is based on sound principles—namely, arterial tracer concentration is relatively constant between the LA and thoracic aorta (physiology) but differentially recovered by the PET scanner due to partial volume effects, motion, and spillover (imaging physics). The variation in absolute flow among AI locations is a distinct concept from changes due to measurement equipment and/or unimportant, short-term biological fluctuations. We have previously explored these issues of repeatability (13).

## CONCLUSIONS

The best customized site for AI activity varies for each patient among the LA, HAo, BAo, or DA. Selection of the customized arterial site for each
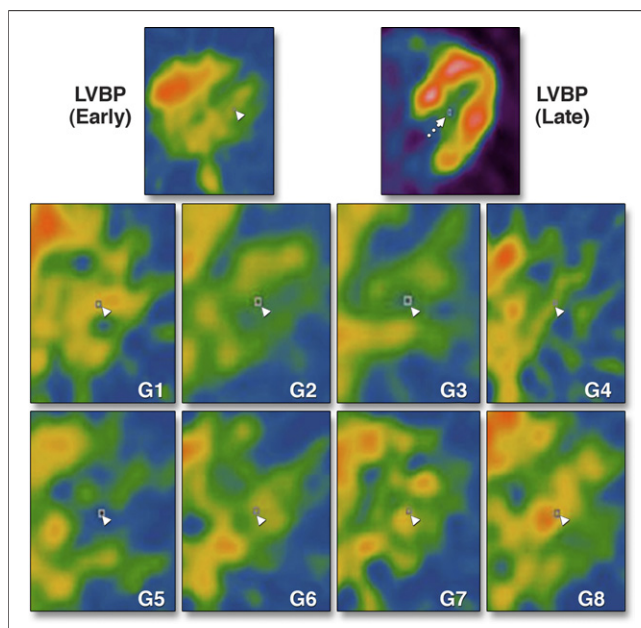


**Figure 6. Gated Images of Fixed AI Location But Moving Myocardium**

Gated first-pass images using a fixed central LV ROI copied from late myocardial uptake. LVBP (Late) = LV late myocardial uptake image with central ROI; LVBP (Early) = 2-min first-pass image with ROI copied from the late myocardial uptake image. First-pass electrocardiography gated images separated into 8 consecutive bins for each cardiac cycle (G1–G8). **Dotted arrow** indicates 2.5-mm ROI placed in the center of the LV on late myocardial uptake image; **arrowhead** indicates ROI copied from the late myocardial uptake image into the first pass image. Abbreviations as in Figure 2.

individual improved quantification of myocardial perfusion in absolute units and CFR with less variability compared with utilizing a single, preselected, fixed anatomic site for AI function.

**Reprint requests and correspondence:** Dr. K. Lance Gould, Weatherhead PET Center For Preventing and Reversing Atherosclerosis, University of Texas Medical School at Houston, 6431 Fannin Street, Room 4.256 MSB, Houston, Texas 77030. *E-mail: K.Lance.Gould@uth.tmc.edu.*

## REFERENCES

1. Tonino PA, De Bruyne B, Pijls NH, et al, for the FAME Study Investigators. Fractional flow reserve versus angiography for guiding percutaneous coronary intervention. N Engl J Med 2009;360:213–24.

2. Johnson NP, Gould KL. Physiological basis for angina and ST-segment change: PET-verified thresholds of quantitative stress myocardial perfusion and coronary flow reserve. J Am Coll Cardiol Img 2011;4:990–8.

3. Johnson NP, Gould KL. Integrating noninvasive absolute flow, coronary flow reserve, and ischemic thresholds into a comprehensive map of physiological severity. J Am Coll Cardiol Img 2012;5:430–40.

4. Bergmann SR, Herrero P, Markham J, Weinheimer CJ, Walsh MN. Noninvasive quantitation of myocardial blood flow in human subjects with oxygen-15-labeled water and positron emission tomography. J Am Coll Cardiol 1989;14:639–52.

5. Bettinardi V, Danna M, Savi A, et al. Performance evaluation of the new whole-body PET/CT scanner: Discovery ST. Eur J Nucl Med Mol Imaging 2004;31:867–81.

6. Gould KL, Pan T, Loghin C, Johnson NP, Sdringola S. Reducing radiation dose in rest-stress cardiac PET/CT by single poststress cine CT for attenuation correction: quantitative validation. J Nucl Med 2008;49:738–45.

7. Yoshida K, Mullani N, Gould KL. Coronary flow and flow reserve by PET simplified for clinical applications using rubidium-82 or nitrogen-13-ammonia. J Nucl Med 1996;37: 1701–12.

8. Johnson NP, Sdringola S, Gould KL. Partial volume correction incorporating Rb-82 positron range for quantitative myocardial perfusion PET

based on systolic-diastolic activity ratios and phantom measurements. J Nucl Cardiol 2011;18:247–58.

9. Hove JD, Iida H, Kofoed KF, Freiberg J, Holm S, Kelbaek H. Left atrial versus left ventricular input function for quantification of the myocardial blood flow with nitrogen-13 ammonia and positron emission tomography. Eur J Nucl Med Mol Imaging 2004;31: 71–6.

10. Herrero P, Markham J, Shelton ME, Bergmann SR. Implementation and evaluation of a two-compartment model for quantification of myocardial

perfusion with rubidium-82 and positron emission tomography. Circ Res 1992;70:496–507.

11. Herrero P, Hartman JJ, Senneff MJ, Bergmann SR. Effects of time discrepancies between input and myocardial time-activity curves on estimates of regional myocardial perfusion with PET. J Nucl Med 1994;35:558–66.

12. Iida H, Rhodes CG, de Silva R, et al. Use of the left ventricular time-activity curve as a noninvasive input function in dynamic oxygen-15-water positron emission tomography. J Nucl Med 1992;33:1669–77.

13. Sdringola S, Johnson NP, Kirkeeide RL, Cid E, Gould KL. Impact of unexpected factors on quantitative myocardial perfusion and coronary flow reserve in young, asymptomatic volunteers. J Am Coll Cardiol Img 2011;4:402–12.